

Two-phase Flow Across Small Diameter Split U-type Junctions

I. Y. Chen*, C. W. Tsai*, B. C. Yang **, C. C. Wang**

*Mechanical Engineering Department, National Yunlin University of Science and Technology, Yunlin, Taiwan 640;
cheniy@yuntech.edu.tw, g9211703@yuntech.edu.tw

**Energy & Resources Laboratories, Industrial Technology Research Institute, Hsinchu, Taiwan 310;
bcyang@itri.org.tw, ccwang@itri.org.tw

ABSTRACT

This study provides qualitatively visual observation of two-phase flow pattern and accurate flowrate measurement for air-water mixture across two horizontal glass tubes with the presence of a vertically split U-type Junction. The diameter of the tubes is 2.7 mm. The curvature ratios ($2R/D$) are 3 and 7 for the U-type junctions. The total mass flux (G) is ranged from 100 to 700 $\text{kg/m}^2\cdot\text{s}$ and quality (x) is changed from 0.001 to 0.5.

The ratio of liquid distribution between the upper and lower outlet legs is related to the inlet flow pattern, but its influence is getting smaller at higher mass flux. The difference of liquid flow rates in the lower and upper legs is significantly affected by gravity at small inlet mass flux, but this difference is getting smaller as inlet mass flux increases. The difference between the water fluxes of upper and lower legs is reduced for smaller curvature radius because the gravity effect is smaller with shorter height difference between the upper and lower legs. However, there is no consistent trend of air flow distribution across the U-type junction as compared to liquid flow distribution. The air mass fluxes in the upper and lower legs always increase with the increases of gas quality and the total mass flux.

INTRODUCTION

Two-phase flow through curved tubes and tees is widely encountered in many industrial heat exchanging applications, such as the steam-power, nuclear and petrochemical plants, and refrigeration and air-condition systems. The curved tubes may be either functioned as a connection tube or as a heat transfer surface, while the tee is utilized as a junction for flow distributing into the two legs of its downstream or as a merger for two flow streams. The design is commonly seen in the heat exchangers of the HVAC &R systems. The two-phase heat transfer (Cho and Tae, 2000 and 2001) and pressure drop (King et al., 1989) in a return bend were reported much higher than those in a straight tube. This is because the induced secondary flow

has a strong influence on two-phase flow pattern in bends (Dean, 1927). The magnitude of such secondary flow obviously increases with the decrease of bend radius and an increase of fluid velocity. A number of researchers had studied the two-phase flow through return bends (Chen et al., 2004; Wang et al., 2004^a) and tee junctions (Wang et al., 2002). However, no study was relevant to the two-phase flow splitting at a equal-sided impacting U-type junctions.

After splitting through a U-type junction, the flow rate in each branch is almost equal and near 50% as compared to the inlet total mass flow rate if the two outlet legs are in the same horizontal plane. Then the gas and liquid phases could be evenly distributed and the quality at two outlet legs should be the same as the inlet quality. However, a maldistribution of the phases may occur when the flow resistances in both legs are not equal. Since the vertically split U-type junction is commonly installed in the evaporator and condenser of air conditioners for flow distribution. Accordingly the flow pattern change is expected to be very complex within the vertically split U-type junction. Also, the flow rates of vapor and liquid, as well as the flow pattern in the two legs downstream will not be the same as the upstream. In addition, the dramatic change of flow pattern may affect the thermo-hydraulic characteristics significantly. Therefore, understanding the phenomenon with the corresponding flow pattern distribution through the vertically split U-type junctions is essential in the design of the thermofluid system. Unfortunately, knowledge for two-phase pattern distribution in equal-sided vertically split U-type junctions is currently not available.

Recently, the design of high-efficiency residential air-conditioner has employed smaller diameter tube in order to improve the airside performance and to reduce the refrigerant charge into the system (Chen et al., 2001). In view of the lack of the basic information of the two-phase flow across the vertically split U-type junction with small tube diameter, therefore, the objective of this study is to conduct a series air-water two-phase flow tests in two

vertically split U-type glass junctions with an inlet horizontal leg and two horizontal outlet legs, having 2.7 mm diameter (D) with two curvature ratios ($2R/D$) of 3 and 7, to investigate the related two-phase flow pattern distribution. Attempts are focused on the observation of the flow pattern change through the equal sided vertically split U-type junction. The flow rates at the upper and lower tubes after the junction are also measured to investigate the influences of the gravity and two-phase flow pattern to the flow rate distribution. The information obtained regarding to the two-phase flow distribution across the vertically split U-type junctions may be valuable for more sophisticated flow regime mapping in the future.

EXPERIMENT METHOD

In this study, air and water are used as the working fluids because air and water have diverse difference of physical properties. The test rig is therefore designed to conduct tests with air-water two-phase mixtures as shown in Fig. 1.

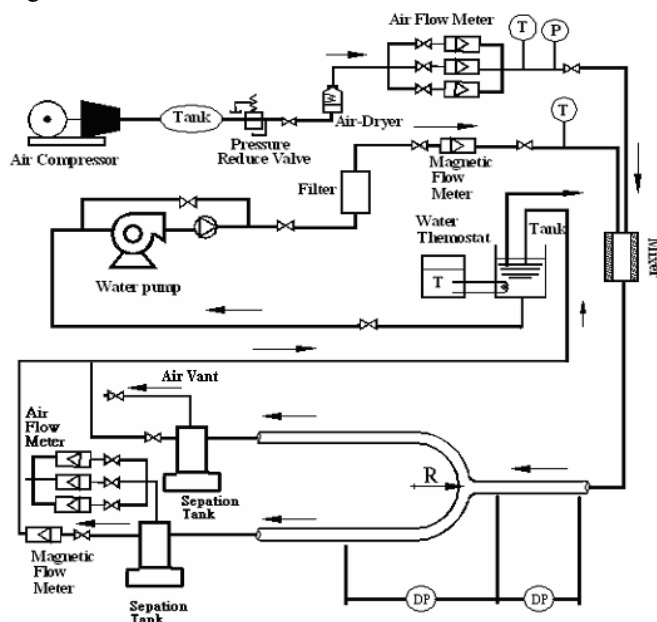


Fig. 1 Schematic of the test rig.

Air is supplied from an air-compressor and then stored in a compressed-air storage tank. Air flow through a pressure reducer, and depending on the mass flux range, is measured by an Aalborg[®] mass flow meter. The water flow loop consists of a variable speed gear pump that delivers water. The mixer was designed to provide better uniformity of the flow stream. The inlet temperatures of air and water were conducted at near 25°C. Three very accurate Yokogawa flow meters with different applicable flow ranges are installed at the downstream of the gear pump. The accuracy of the air and water mass flow meters is within $\pm 0.2\%$ of the test span. After splitting through the U-type junction, the mixture flow leaving from each outlet leg, air and water are separated by an open water tank. The separated air and water flow rates from the lower leg are

measured by another sets of Aalborg[®] mass flowmeters and Yokogawa flow meters, and then the air is vented and the water is re-circulated. The air and water temperatures were measured by resistance temperature device (Pt100 Ω) having a calibrated accuracy of 0.1 K (calibrated by Hewlett-Packard quartz thermometer probe with quartz thermometer, model 18111A and 2804A). Detailed description of the test apparatus and the estimated uncertainties of the measurements had been previously reported (Chen et al., 2004; Wang et al., 2004^a)

Two horizontal glass tubes with the presence of two vertically split U-type Junctions having 2.7 mm diameter (D) with two curvature ratios ($2R/D$) of 3 and 7 are utilized for tests. To achieve a fully developed flow condition for visual observation, a straight entrance length of $100D$ is located at the upper stream of the inlet leg and an outlet length of $60D$ is located at each downstream leg as shown in Fig. 2. The roughness of the glass tubes is measured by Mahr perthometer (model M4Pi-RK) having an accuracy of 0.01 μm . The mean roughness of glass tubes is less than 0.04 μm .

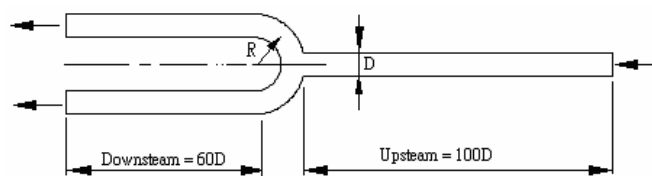


Fig. 2 Schematic of the vertically split U-type junction.

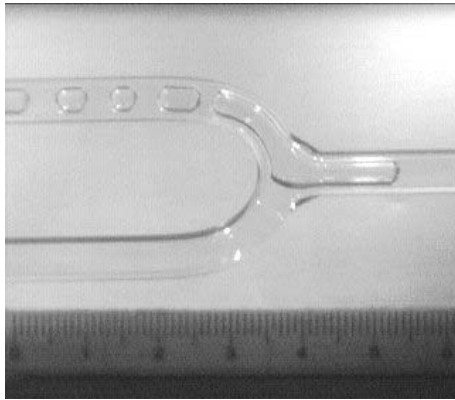
The total mass flux (G) is ranged from 100 to 700 $\text{kg/m}^2\text{-s}$ and quality (x) is changed from 0.001 to 0.5. Observations of flow patterns are obtained from images produced by a high speed camera of Redlake Motionscope PCI 8000s. The maximum camera shutter speed is 1/8000 second. The high speed camera is positioned to obtain the side views of the vertically split U-type junction, the upstream and downstream legs.

RESULTS AND DISCUSSION

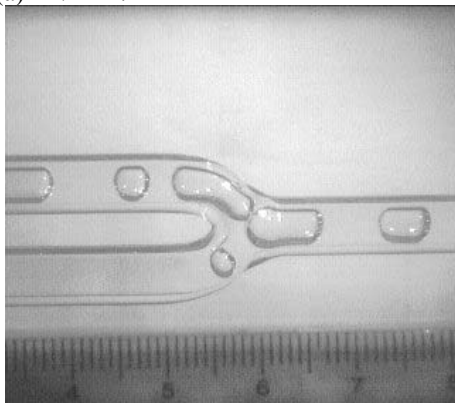
Flow Pattern Observation

Photographs that are representative of the observed flow patterns for both tubes ($2R/D = 3$ and 7) at $G = 100\text{kg/m}^2\text{s}$ and $x = 0.001$ are shown in Fig. 3. The flow pattern at the upstream is plug flow. As the plug approaches the vertically split junction, the air plug is slow down and merges with the front air plug into a longer plug. Most air flow goes to the upper leg by the buoyancy force and large portion of the liquid flows to the lower leg due to the gravity force. A small portion of liquid is carried to the upper leg by the inertial force of the air plug. The flow pattern in the upper leg is still plug flow; however, the lower leg becomes single bubble flow. In addition, the plug is temporarily pending at the junction by the buoyancy force

for a short time. This freezing slug was also observed in vertical return bends (Wang et al., 2004^b).

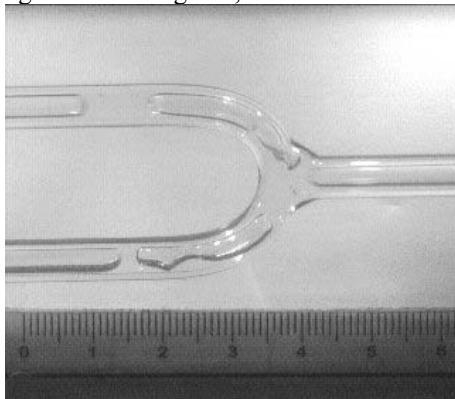


(a) $2R/D = 7$

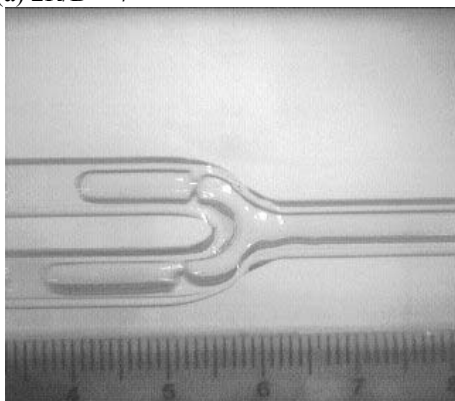


(b) $2R/D = 3$

Fig. 3 $G = 100 \text{ kg/m}^2\text{s}$, $x = 0.001$



(a) $2R/D = 7$

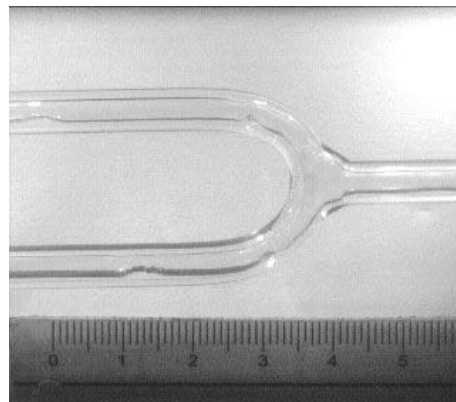


(b) $2R/D = 3$

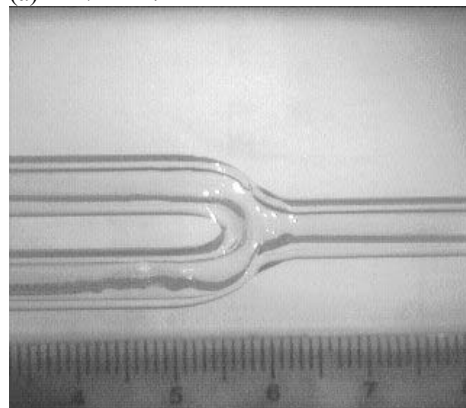
Fig. 4 $G = 100 \text{ kg/m}^2\text{s}$, $x = 0.009$

As x increases to 0.009, the flow photos are shown in Fig. 4. The inlet flow pattern changes to slug flow with a long air slug following a liquid slug. For a smaller diameter tube, the influence of surface tension is comparatively large and the air slug can easily occupy the whole cross section, even at the split of the junction. Also, the splashing liquid shown as ripple spreads around the periphery of the bend by the centrifugal force in the U-type split junction. Thus, the liquid distributed to the upper leg becomes more close to the liquid flowing to the lower leg, obviously shown in Fig. 4-b. The flow patterns in both outlet legs are still slug flow, but their length is less than the inlet slug.

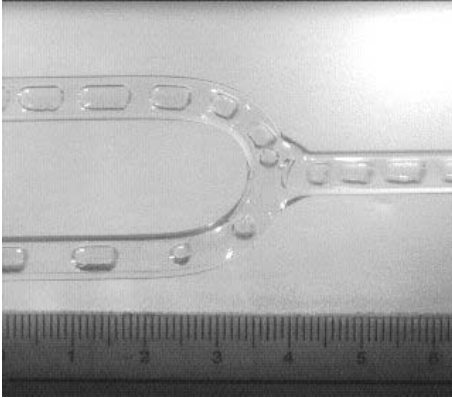
With further increase of the gas quality to 0.05 at $G = 100 \text{ kg/m}^2\text{s}$, the flow speed becomes higher as shown in Fig. 5. The inlet flow pattern becomes stratified flow, more liquid flows down to the lower tube by the gravity; only a small portion of liquid is carried to the upper leg by airflow. Due to the centrifugal force, the liquid ripple is seen swirled around the periphery in the split U-type junction to form a temporary annular flow in the split U-type junction. However, this phenomenon is not existed too far as compared to the temporary annular flow observed for stratified flow across U-type bends (Wang, et al., 2003). The flow pattern in the upper leg changes to stratified flow while the wavy stratified flow is seen in the lower leg by the higher liquid flow. As the gas quality is further increased, the inlet flow pattern changes to annular flow. The flow pattern remains unchanged across the split U-type junction.



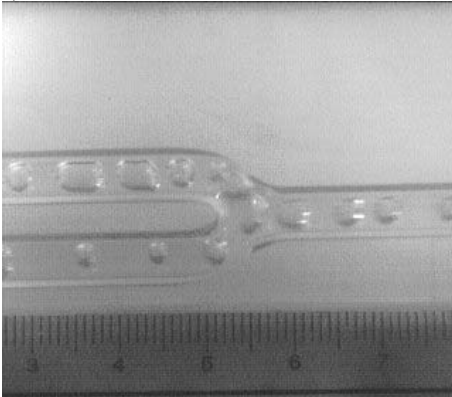
(a) $2R/D = 7$



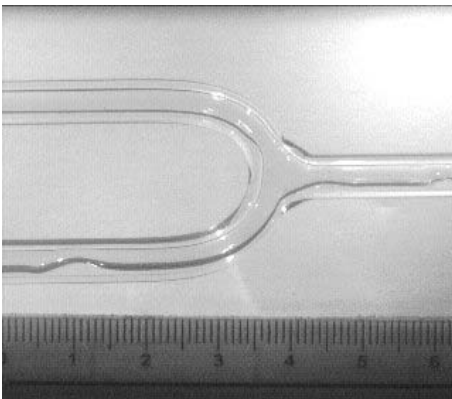
(b) $2R/D = 3$
 Fig. 5 $G = 100 \text{ kg/m}^2\text{s}$, $x = 0.05$



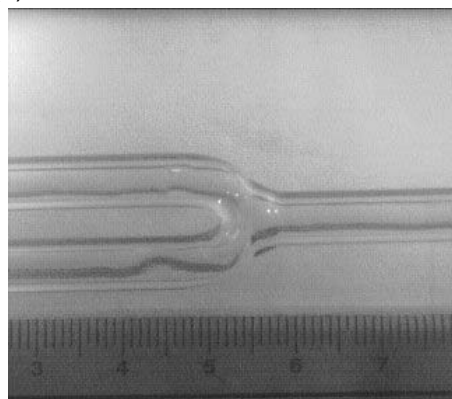
(a) $2R/D = 7$



(b) $2R/D = 3$
 Fig. 6 $G = 300 \text{ kg/m}^2\text{s}$, $x = 0.001$



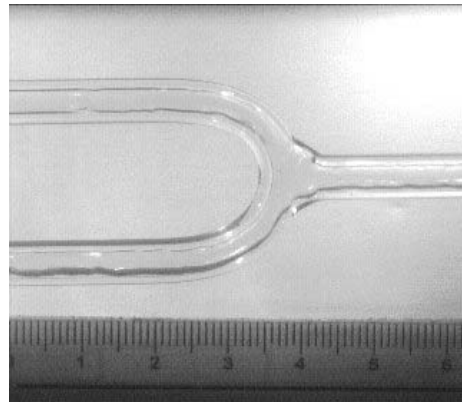
(a) $2R/D = 7$



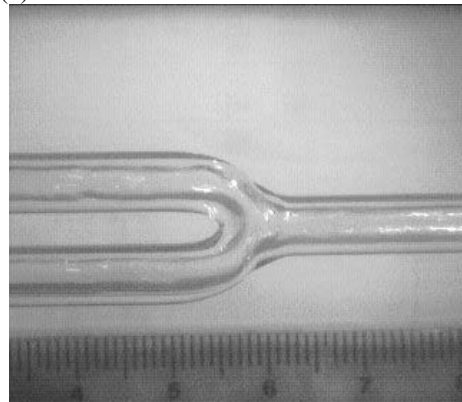
(b) $2R/D = 3$
 Fig. 7 $G = 300 \text{ kg/m}^2\text{s}$, $x = 0.009$

As the mass flux is further increased to $300 \text{ kg/m}^2\text{s}$, the inertia force takes over the influence of gravity force. For $x = 0.001$ (Fig. 6), the inlet flow pattern is plug flow with the bubble size near the tube diameter. As the air plug reaches the split U-type junction, its speed is reduced by the buoyancy force but the plugs do not merge into a large one at the split junction like $G = 100 \text{ kg/m}^2\text{s}$. As the flow passes the junction, more liquid goes to the lower leg and most of air plugs flow to the upper leg. Thus, the flow pattern changes to bubbly flow in the lower leg while the flow in the upper leg still maintains the plug flow.

As the gas quality increases to $x = 0.009$, the inlet flow changes to wavy stratified flow (Fig. 7). When the higher liquid reaches the split junction, it will directly impact the convex part of the U-type bend. Part of the liquid flow is pushed to the convex surface of the upper bend, and then the liquid is swirled up around the periphery to form a temporary annular flow in the U-type split junction. The temporary annular flow eventually returns back to stratified flow at the downstream region of the upper leg. Since most of the liquid flow goes down to the lower leg, the wavy stratified flow is still observed in the lower tube, but the flow pattern sometime may change to slug flow as the wavy liquid hits the top of the tube.



(a) $2R/D = 7$



(b) $2R/D = 3$
 Fig. 8 $G = 300 \text{ kg/m}^2\text{s}$, $x = 0.09$

As gas quality further increases to $x = 0.09$ (Fig. 8), the inlet flow pattern becomes semi-annular flow. As the flow across the split junction, the gas inertial force still high such that the flow patterns in the upper and lower legs remain in semi-annular flow. As the gas quality further increased, the inlet flow pattern becomes annular flow. The flow pattern maintains unchanged across the split U-type junction. The air and water flow rates seem more evenly distributed in the upper and lower legs.

Flowrates Distribution

Fig. 9 shows air and water fluxes having $2R/D = 7$ and $G = 100 \text{ kg/m}^2\text{-s}$ versus gas quality x . For $x = 0.001$ to 0.009 , the inlet flow pattern is intermittent flow. As flow across the vertically split U-type junction with increasing gas quality, more and more liquid is carried to the upper leg by the higher air inertial force. As x is increased from 0.01 to 0.09 , the inlet flow pattern is changed from intermittent flow to stratified flow. As seen the corresponding water flux of the lower leg is gradually increased because more liquid falls into the lower leg at the split junction by the gravity force without directly hitting the convex surface of the U-type bend. As x further increases from 0.09 to 0.5 , the flow pattern changes to semi-annular flow then annular flow. Since the gas inertial force does not dominate the flow rate distribution for small mass flux even at higher gas quality, therefore, the liquid flow rate in the lower leg is still much greater than the upper leg by the gravity force.

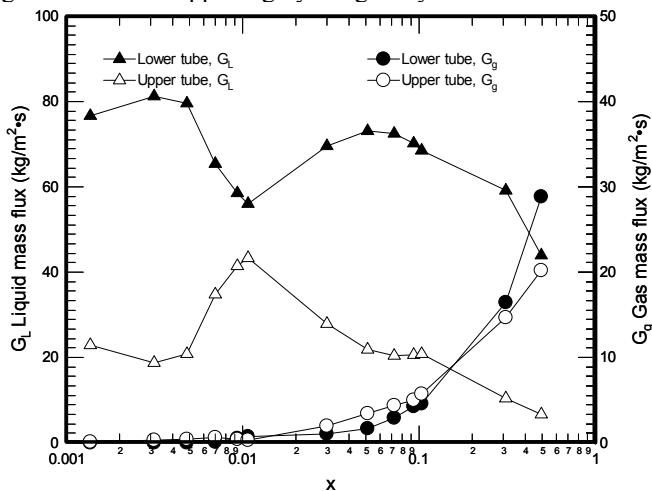


Fig. 9. Air and water mass flux vs. x for $2R/D = 7$, $G = 100 \text{ kg/m}^2\text{-s}$.

As mass flux G increased to $300 \text{ kg/m}^2\text{-s}$ and $G = 700 \text{ kg/m}^2\text{-s}$, the curves of the air and water mass fluxes in the outlet legs shown in Figs. 10 and 11, respectively. At higher mass flux, the gravity effect is reduced by the inertial and surface tension forces such that the gas and liquid flow rates become closer in the upper and lower legs. In addition, the friction resistance becomes greater at higher mass flux and gas quality, it can make the flow rates of gas and liquid more evenly distributed in both legs especially for $G = 700 \text{ kg/m}^2\text{-s}$.

The air and water flow curves in the upper and lower outlet legs for $2R/D = 3$ having $G = 100$, 300 and $700 \text{ kg/m}^2\text{-s}$ are shown Figs. 12-14, respectively. Obviously, the difference between the water fluxes of upper and lower legs is smaller for $2R/D = 3$ which is caused by the smaller height difference between the upper and lower legs. In addition, the liquid flow rate in the upper leg is greater than the lower leg which is only observed at $G = 700 \text{ kg/m}^2\text{-s}$ and $x > 0.05$ which shows the gravity effect is less than the surface tension and inertial force at this condition.

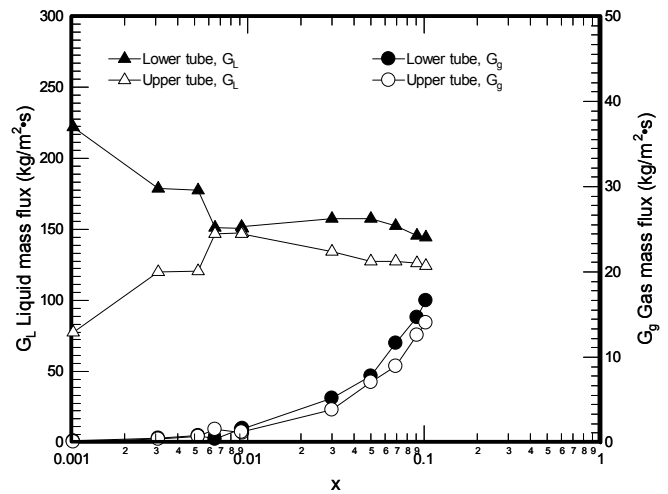


Fig. 10. Air and water mass flux vs. x for $2R/D = 7$, $G = 300 \text{ kg/m}^2\text{-s}$.

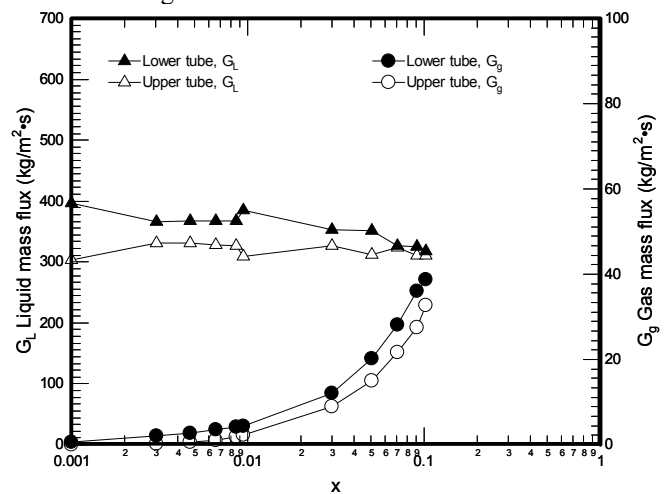


Fig. 11. Air and water mass flux vs. x for $2R/D = 7$, $G = 700 \text{ kg/m}^2\text{-s}$.

From the flow distribution shown in Figs. 9-14, the liquid flow rate distribution for the upper and lower legs is found greatly related to the inlet flow pattern and curvature radius. Higher liquid flow rate into the lower leg and smaller liquid flows to the upper leg, especially for lower mass flux, are observed due to the gravity force. This is caused by the height difference between the upper and lower legs. As compared to the results shown in Figs 9-11 for $2R/D = 7$ and Figs. 12-14 for $2R/D = 3$, the trends of the air and water flow curves for curvature ratios of 7 and 3 seem very similar. However, the liquid flow difference between the upper and lower legs in this study for $D = 2.7$

mm is relatively smaller as compared to the results shown in vertically U-type junctions with $D = 6.7$ mm (Chen et al., 2005) due to the higher surface tension effect and smaller gravity influence.

For the air flow curves of the upper and lower legs as shown in Figs. 9-14, there is no consistent trend as the liquid flow curves, however, the mass fluxes in the upper and lower legs always increase with the increases of x and G .

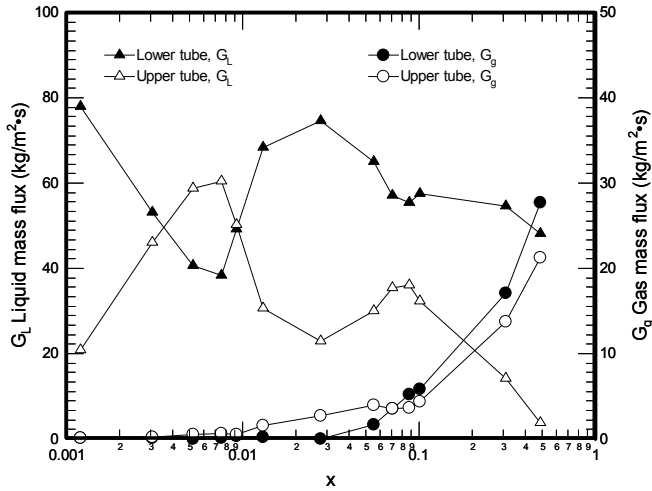


Fig 12. Air and water mass flux vs. x for $2R/D = 3$, $G = 100$ $\text{kg/m}^2\text{s}$.

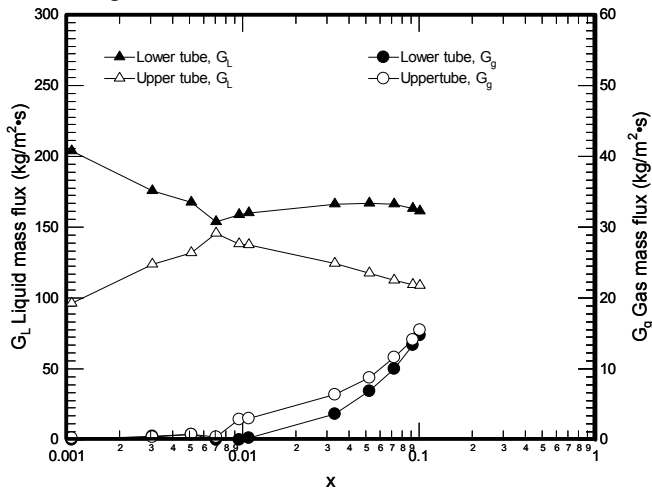


Fig 13. Air and water mass flux vs. x for $2R/D = 3$, $G = 300$ $\text{kg/m}^2\text{s}$.

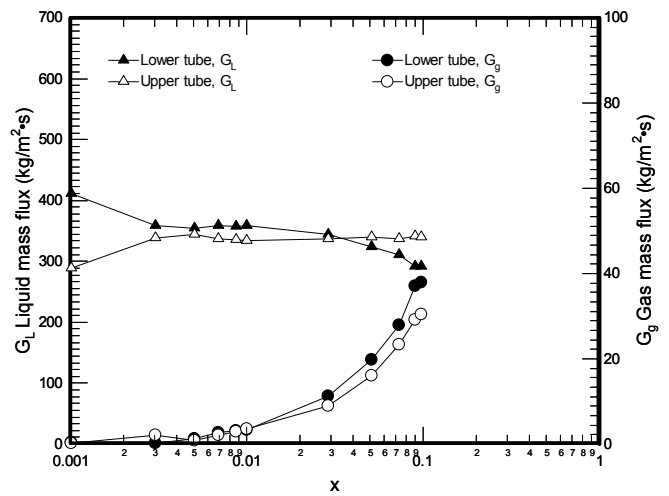


Fig 14. Air and water mass flux vs. x for $2R/D = 3$, $G = 700$ $\text{kg/m}^2\text{s}$.

CONCLUSION

1. Stratified flow is almost not observed in this study because the effect of the surface tension is greater in small tube.
2. Due to the centrifugal force, the liquid ripple is seen swirled around the periphery of the split U-type junction in the slug and stratified flow regions.
3. The ratio of liquid distribution between the upper and lower outlet legs is related to the inlet flow pattern, but its influence is getting smaller at higher mass flux.
4. The difference of liquid distribution in the lower and upper legs is significantly affected by gravity at small inlet mass flux, but this difference is getting smaller as inlet mass flux increases.
5. The difference between the water fluxes of upper and lower legs is reduced for smaller curvature radius because the gravity effect is smaller with shorter height difference between the upper and lower legs.

ACKNOWLEDGE

The authors would like to acknowledge the financial supports provided by the Energy Commission of the Ministry of Economic Affairs, Taiwan, R.O.C. and National Science Council (NSC 90-2212-E-224-006).

REFERENCE

1. Chen, I. Y., Yang, K. S., and Wang, C. C., 2001, Two-Phase Frictional Pressure Drop Correlations for Small Tubes, *J. of Thermophysics and Heat Transfer*, Vol. 15, No. 4, pp. 409-415.
2. Chen, I. Y., Wang, C. C., and Huang, J. C., 2004, Single-phase and Two-phase Frictional Characteristics of Small U-type Wavy Tubes, *Int. Comm. Heat Mass Transfer*, Vol. 31, No. 3, pp. 303-314.
3. Cho, K., and Tae, S. J., 2000, Evaporation Heat Transfer for R-22 and R-407 Refrigerant-oil Mixture

- in a Microfin Tube with a U-bend, *Int. J. of Refrigeration*, vol. 23, pp. 219-231.
4. Cho, K., and Tae, S. J., 2001, Condensation Heat Transfer for R-22 and R-407 refrigerant-oil mixtures in a microfin tube with a U-bend, *Int. J. of Heat Mass Transfer*, vol. 44, pp. 2043-2051.
 5. Dean, W. R., 1927, Note on the Motion of Fluid in Curved Pipe, *Phil. Mag.* Vol. 4, 208-223. Vol. 28, pp. 2007-2016.
 8. Wang, C. C., Chen, I. Y., Yang, Y. W., and Chang, Y. J., 2003, Two-phase Flow Pattern in Small Diameter Tubes with the Presence of Return Bend, *Int. J. of Heat and Mass Transfer*, Vol. 46, pp. 2975-2981.
 9. Wang, C. C., Chen, I. Y., Yang, Y. W., and Hu, R., 2004^a, Influence of Horizontal Return Bend on the Two-Phase Flow Pattern in Small Diameter Tubes, *Exp. Thermal Fluid Sci.*, Vol. 28, pp. 145-152.
 6. King, J. S., Katsuy, N., Masafumi, K., Kouichiro, K., and Toshiaki, H., 1989, Influence of Oil on Refrigerant Evaporator Performance, 4th Report: Flow Regime and Pressure Drop in Return Bend,” *Transactions of the JAR*, Vol. 6, No. 1, pp. 79-89.
 7. Wang, S., and Shoji, M., 2002, Fluctuation Characteristics of Two-Phase Flow Splitting at a vertical impacting T-junction, *Int. J. Multiphase Flow*,
 10. Wang, C. C., Chen, I. Y., and Huang, P. S., 2004^b, Influence of Vertical Return Bend on the Vapor Slug Velocity, *Int. J. Heat and Mass Flow* (under review).
 11. Chen, I. Y., Tsai, C. W., Hu, R., and Wang, C. C., 2005, Air-Water Two-phase Flow Across Vertically Split U-type Junctions, *6th World Conference on Experimental Heat Transfer, Fluid Mechanics, and Thermodynamics*, April 17-21, 2005, Miyagi, Japan.